J Mater Sci: Mater Med (2008) 19:1905–1911
DOI 10.1007/s10856-007-3260-x

Improvement in crystallinity of apatite coating on titanium with the insertion of CaF_2 buffer layer

Su-Hee Lee · Hyoun-Ee Kim · Hae-Won Kim

Received: 24 October 2006 / Accepted: 9 July 2007 / Published online: 4 October 2007

Abstract In the apatite coatings on Ti the heat treatment process is necessary to crystallize the apatite structure for improved chemical stability and biological properties. However, the heat treatment normally degrades the mechanical strength of the coating layer associated with thermally induced stress. In this study, we aimed to improve the crystallization of apatite coating by using calcium fluoride (CaF_2) as a buffer layer. The insertion of a thin layer of CaF_2 (0.2–1 μm) between apatite and Ti significantly improved the crystallization behavior of apatite. Moreover, this crystallization was more enhanced as the thickness of CaF_2 was increased. When a 1 μm-thick CaF_2 was inserted, the crystallization of apatite initiated at a temperature as low as 320 °C, being a dramatic improvement in the crystallization when considering the crystallization initiation temperature of a bare apatite coating on Ti was ~450 °C. As a result of this crystallization enhancement, the dissolution behavior of CaF_2-inserted apatite coatings was more stable than that of the bare apatite coating, showing much reduced initial-burst effect. Preliminary cellular assay showed the CaF_2-inserted apatite coating provided a substrate for cells to spread and grow favorably, as being similar to the bare apatite coating. This novel way of apatite coating on Ti using CaF_2 buffer layer may be useful in the coating systems particularly requiring low temperature processing and increased crystallinity with high chemical stability.

S.-H. Lee · H.-E. Kim
School of Materials Science and Engineering,
Seoul National University, Seoul 151-744, Korea

H.-W. Kim (✉)
Department of Biomaterials Science, School of Dentistry,
Dankook University, Cheonan 330-714, Korea
e-mail: kimhw@dankook.ac.kr

1 Introduction

Titanium (Ti) and its alloys have long been recognized as potential implant materials in dentistry and orthopedics. In order to improve the implant-tissue osseointegration, significant effort has been made to tailor the surface of Ti either physically or chemically or both. Among the surface modifications, apatite coatings on Ti have been shown to allow rapid bone growth to the implants and intimate contact of bone-implant. The improved biocompatibility driven by the apatite coatings was mainly attributed to the chemical and biological affinity of apatite to host tissues, as well as its osteoconductivity. Conventionally, apatite coatings were carried out by a plasma spraying technique [1]. However, the plasma-sprayed apatite coating is known to be inhomogeneous in structure and to hold stress and even cracks due to the high-temperature processing and thick coating layer [2, 3]. As alternative coating techniques, sol-gel method [4, 5], biomimetic immersion [6], electrochemical deposition [7], sputtering [8, 9], ion-beam deposition [10], and electron-beam (e-beam) evaporation [11, 12] have been developed.

The authors have recently reported a series of works on the e-beam deposited apatite [11, 12]. Thus obtained apatite layer was thin (hundreds nanometers to few micrometers) and the thickness was easily controlled. Moreover the e-beam deposited apatite retained high structural purity and good bond strength (~40 MPa). However, the as-deposited coating was still in an amorphous state, therefore post heat-treatment was inevitable. Our previous study has shown the threshold temperature for the apatite crystallization was around 450 °C when deposited directly on Ti. This crystallization step was necessary for the coating layer to retain chemical stability. When the coated film was not crystallized, it dissolved so

rapidly as to direct harmful cellular responses [13]. However, as the crystallization process is normally performed at elevated temperatures, it results in mechanical degradation of the coating layer. Principally, thermal stress is developed within the coating layer due to the thermal mismatch between apatite and metallic substrate. More severe is that the coating layer often holds cracks after crystallization, and this is more conspicuous with increasing coating thickness. Although the coating layer does not show appearance of cracks, the tensile bond strength of the coatings is significantly reduced by the crystallization [11, 12].

Therefore, it would be better to reduce crystallization temperature of the apatite as low as possible. The improvement in crystallization of apatite is also beneficial in the aspect of processing cost. In this study, the authors aimed to improve the crystallization of apatite in the e-beam process through the insertion of an intermediate buffer layer. We used calcium fluoride (CaF_2) as the buffer layer. Recently our group observed an unusual crystallization behavior of CaF_2, i.e., it was crystallized even at room temperature without subsequent heat treatment [14]. Moreover, the CaF_2 coating was observed to be nontoxic but to improve the growth level of the MG63 osteoblastic cells [14]. At a glance consideration, CaF_2 is known to induce the formation of fluoridated apatite in vivo [15]. Moreover, fluoride is known to improve the crystallization of apatite [16]. Taken these together, the CaF_2 is considered to be formed easily as a buffer layer without degrading Ti substrate associated with thermal process, and the predeposited CaF_2 layer is believed to play some role in the crystallization of apatite.

Herein we report the effect of CaF_2 buffer layer on the crystallization of an apatite coating on Ti and the consequent dissolution behavior. Preliminary cell response to the coating layer is also briefly assessed.

2 Materials and methods

2.1 Preparation of coatings

Commercially pure Ti (CP-Ti, grade 4) was used as a substrate. Ti substrates cut to a dimension of 10 mm × 10 mm × 2 mm were ground with SiC paper (grit# 1000), followed by ultrasonic cleaning in acetone, ethanol and distilled water each for 10 min. Using the e-beam apparatus (EVACO-EB700R, DR Vacuum Co, Ltd., Korea), the CaF_2 target prepared as a block was evaporated onto the Ti substrates at the rate of 0.6–0.7 nm/s. The thickness of the CaF_2 was varied (0.2, 0.5 and 1.0 μm). On the predeposited CaF_2, apatite was deposited using the same apparatus. The target for the apatite was prepared following our previous recipe wherein additional CaO was mixed with pure apatite (apatite:CaO = 3:1 by weight) in order to adjust the deposited apatite film to the apatite stoichiomerty (Ca/P = 1.67), which was derived from the different vapor pressures of Ca and P [12]. The apatite layer has a thickness of 1.0 μm. As the apatite was still in amorphous state, heat treatment was subjected on the apatite/CaF_2 coating at various temperatures (300–500 °C) for 1 h. Table 1 summarizes the thicknesses and designations of the apatite/CaF_2 films prepared in this study.

Table 1 Types of the apatite coatings without and with insertion of CaF_2 with varying thickness, and their designations

Designation	Coating layer (thickness)
HA	HA(1.0 μm)
HA/CF2	HA(1.0 μm)/CaF_2(0.2 μm)
HA/CF5	HA(1.0 μm)/CaF_2(0.5 μm)
HA/CF10	HA(1.0 μm)/CaF_2(1.0 μm)

2.2 Characterization of coatings

The phase of the coatings was analyzed by X-ray diffraction (XRD; M18XHF, Mac Science, Japan) to observe the crystallization behavior. The morphology of the coating was observed using field emission scanning electron microscopy (SEM; JSM6330F, JEOL, Japan). Dissolution behavior of the coatings was monitored in a physiological saline solution. Each specimen was inserted in a vial containing 5 ml of the solution and held at 37 °C. The solution was refreshed every day. At predetermined time points, sample was taken out and the solution was analyzed using inductively coupled plasma atomic emission spectroscopy to determine the eluted concentration of Ca ions (ICP-AES; ICPS-7500, SHIMADZU, Japan).

Preliminary cell response to the coatings was observed. MC3T3-E1 preosteoblast was cultured in a humidified atmosphere of 5% CO_2/95% air at 37 °C. Specimens for the cell tests (HA, HA/CF2, HA/CF5, and HA/CF10) were rinsed in 70% ethanol and dried. The cells were plated at a density of 6×10^4 cells/ml on the specimens contained in individual wells of a 24-well plate. After culturing for 3 days the cell morphology was observed with SEM at an accelerating voltage of 10 kV, after fixing the cells with 2.5% glutaraldehyde, dehydrating with a series of graded ethanols (70, 90, and 100%) and critical point drying with CO_2.

3 Results and discussion

3.1 Crystallization and morphology of coatings

Figure 1(A–D) shows the XRD patterns of the apatite coatings without and with the insertion of CaF_2 buffer layer

with different thicknesses. When apatite was deposited directly on Ti (Fig. 1A), crystallization was observed to initiate at 450 °C, which well corresponded to our previous work. The CaF_2 was pre-deposited on Ti with varying thickness and then apatite was coated on this CaF_2-coated Ti (Fig. 1B–D). The pre-deposited CaF_2 was easily crystallized at room temperature when deposited on Ti. Importantly, the insertion of CaF_2 thin layer was observed to decrease the crystallization temperature significantly. The crystallization of apatite initiated as low as 320 °C with the insertion of CaF_2. Moreover, the apatite peak intensity was more apparent with increasing thickness of CaF_2. When a 1 μm-CaF_2 was inserted the apatite phase was well developed at 320 °C and was even better than that of the bare apatite coating (without the CaF_2 layer) heat treated at 500 °C.

However, the heat treatment of CaF_2-inserted apatite coating at 500 °C resulted in the formation of other phases, such as tetracalcium phosphate (TTCP) and CaO. The appearance of those phases was accompanied by the reduction of CaF_2 and apatite peaks, suggesting that those were attributed to the reaction between CaF_2 and apatite. Therefore, the crystallization temperature of the CaF_2-inserted apatite coating is not considered to be increased as high as the case in the bare apatite coating.

Figure 2 shows the surface morphologies of the apatite coatings without and with the insertion of CaF_2 buffer layer. The bare apatite coating on Ti followed by a heat treatment at 320 °C showed a typical e-beam deposited film morphology (Fig. 2A). This surface image of the e-beam apatite coating was similarly observed without regard to the crystallization temperature. When the apatite was coated on a thin CaF_2 layer and followed by a heat treatment at 320 °C (HA/CF2 coating), a similar surface morphology was observed (Fig. 2B). However, when relatively large thickness of CaF_2 was inserted and heat treated at 320 °C an intriguing grain-like morphology was developed (HA/CF5 and HA/CF10 coatings, in Fig. 2C and D, respectively). The size of each grain-like region was increased with increasing the thickness of CaF_2.

The morphology of the apatite coating was observed with varying the thickness of apatite layer (50–500 nm) on a 1 μm-thick CaF_2 to better understand the development of grain-like morphology, as shown in Fig. 3. The CaF_2 layer showed a morphology consisting of many triangular terraces, as was observed in our previous work (Fig. 3A) [14]. When a 50 nm-thick apatite was deposited on the CaF_2

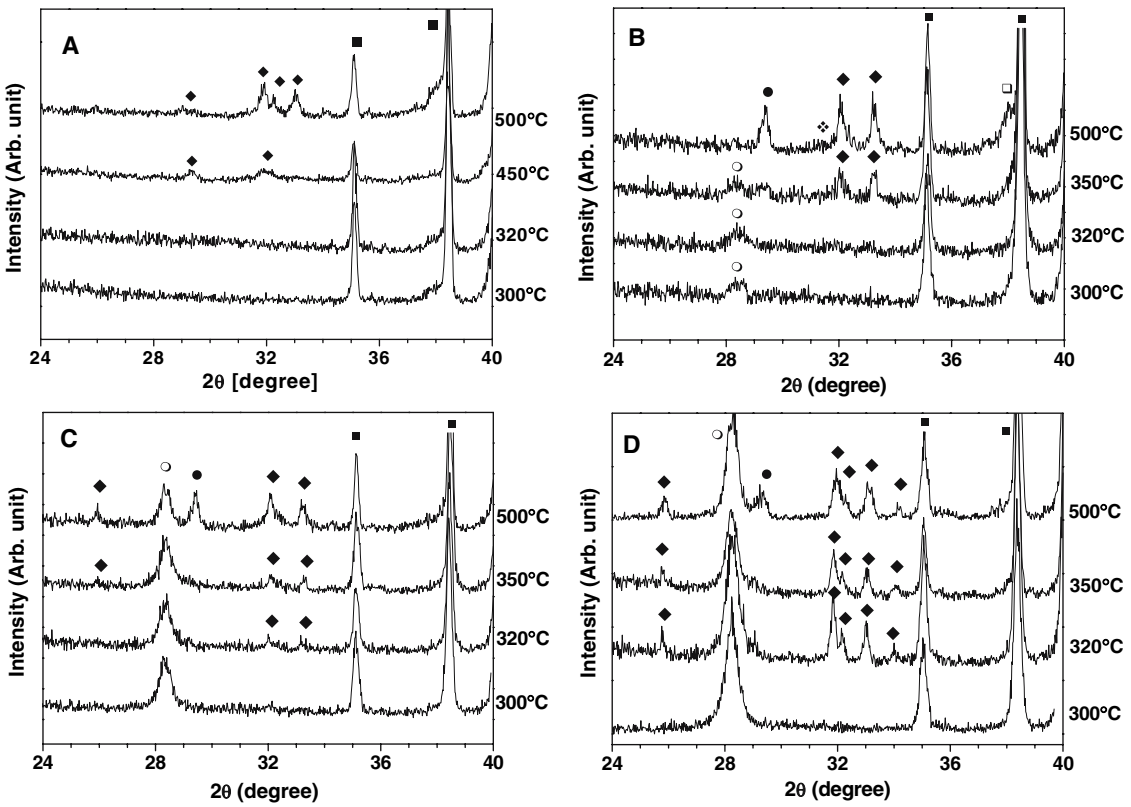

Fig. 1 XRD patterns of the coatings at different heat treatment temperatures:(**A**) HA, (**B**) HA/CF2, (**C**) HA/CF5 and (**D**) HA/CF10. (❍ CaF_2, ◆ HA, ❖ TCP, ● TTCP, ❑ CaO, ■ Ti)

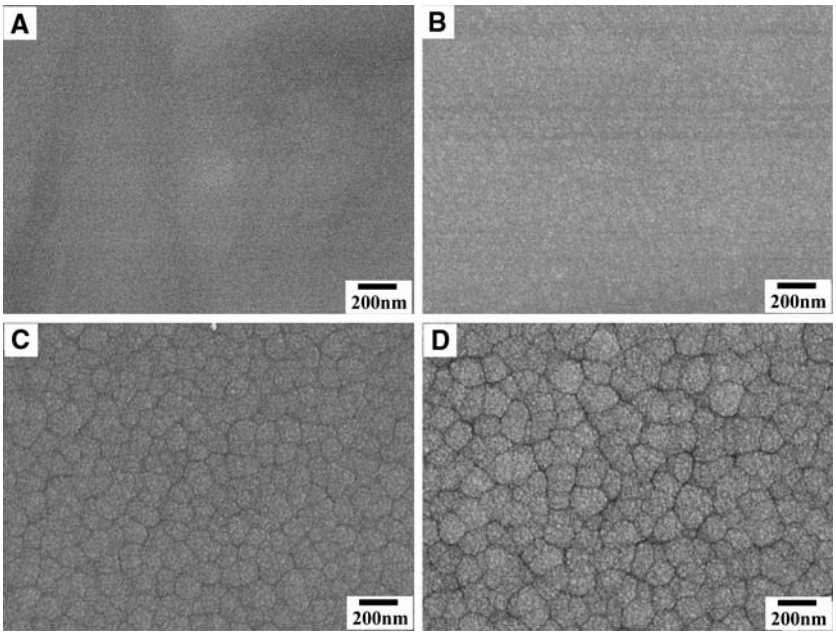

Fig. 2 SEM surface morphologies of the coatings after heat treatment at 320 °C: (**A**) HA, (**B**) HA/CF2, (**C**) HA/CF5 and (**D**) HA/CF10

layer, some of the edges in triangular terraces became blunt although the triangular shape remained to some degree (Fig. 3B). With increasing the thickness of apatite to 200 nm (Fig 3C) all edges in the triangular terraces became completely rounded, showing the development of grain-like morphology on the whole surface. As the apatite thickness was increased to 500 nm, the grain-like regions became larger (Fig. 3D). However, with further increase in the thickness of apatite little difference was observed (compare Fig. 3D with Fig. 2D), suggesting there might exist a threshold thickness of apatite (herein ~500 nm) that determined the stable growth of the grain-like apatite morphology.

The SEM cross-section view of the CaF_2-inserted apatite coating is shown in Fig. 4. The coating layer was observed to be supported well on the Ti substrate, without holding any cracks or delaminations. There appeared to exist some difference in the morphology between apatite and CaF_2, in other words, CaF_2 showed somewhat columnar or granular morphology. Of special to note is that the lower part of the apatite layer in contact with CaF_2 appeared also to be columnar/granular following the

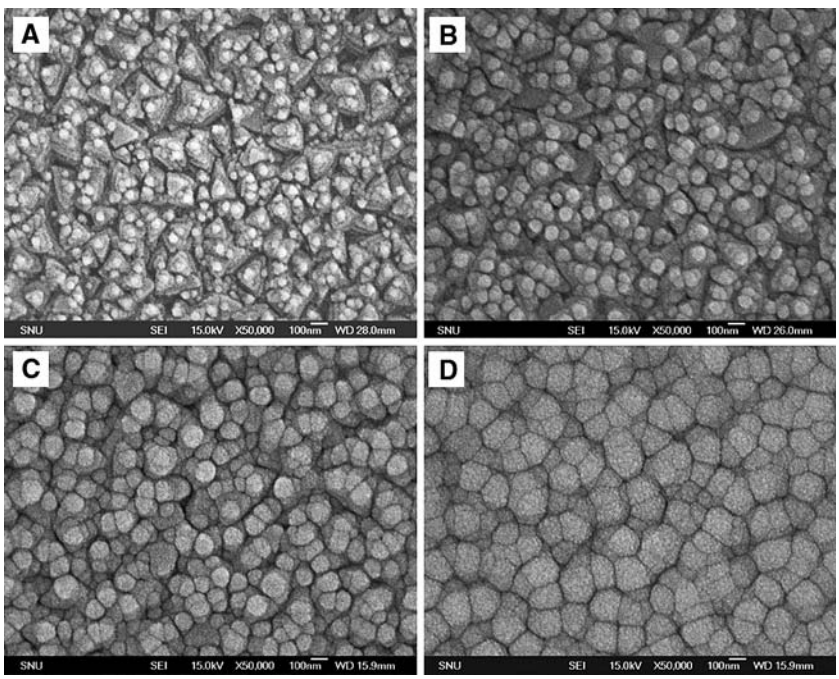

Fig. 3 SEM surface morphologies of the apatite coatings at different thicknesses on a 1 μm-thick CaF_2 layer after heat treatment at 320 °C: (**A**) pure CaF_2, (**B**) 50 nm, (**C**) 200 nm and (**D**) 500 nm apatite

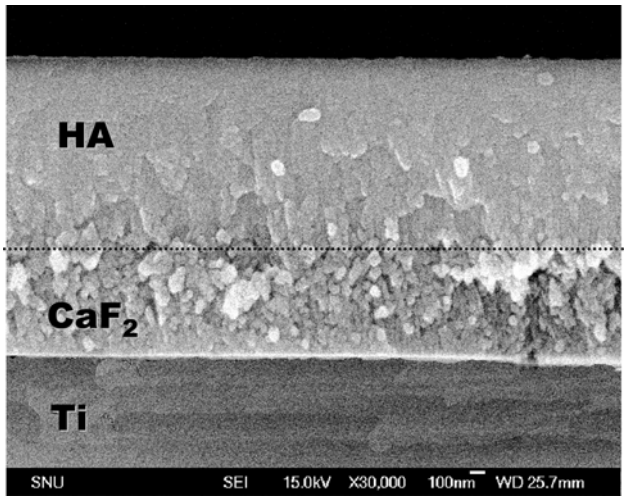

Fig. 4 SEM cross-section view of the apatite coating with inserted CaF_2 layer on Ti. HA/CF5 is presented as a representative image. Coating layer was heat-treated at 320 °C

underlying CaF_2 layer, which suggests the growth of apatite would be influenced by the CaF_2 morphology.

It has been reported that CaF_2 acted as a nucleating agent of apatite in the glass-ceramics [15]. As such, many biomedical grade glass-ceramics contain some concentration of CaF_2 in their initial glass composition to induce crystallization of apatite [17, 18]. It was also observed that increase in the fluoride content decreased the glass transition temperature (T_g), and thus reasoned that fluoride acted as an accelerator of crystallization by enhancing the motion and rearrangement of atoms for the crystallization within the glass network [15, 17]. In this case, the fluorine may take part in the formation of apatite, forming partially-fluoridated apatite. However, in the present study, we could not elucidate whether the apatite layer contains fluorine or not as the detection of fluorine within apatite appears to remain beyond the scope of this study.

For any possible hypotheses, the important thing is that the underlying CaF_2 layer played a crucial role in the crystallization of apatite coating by reducing the crystallization initiation temperature down to ~320 °C. This enhancement in the crystallization should be potentially considered in the production of apatite with better chemical stability at reduced heat treatment temperature and more relieved thermal mismatch as these are importantly considered in the e-beam apatite coatings. In the following section, we explain the enhanced chemical stability of the CaF_2-inerted coatings driven by this crystallization improvement.

3.2 Properties of apatite/CaF_2 coatings

As shown in Fig. 5, the dissolution behavior of the apatite coatings was significantly changed by the insertion of CaF_2

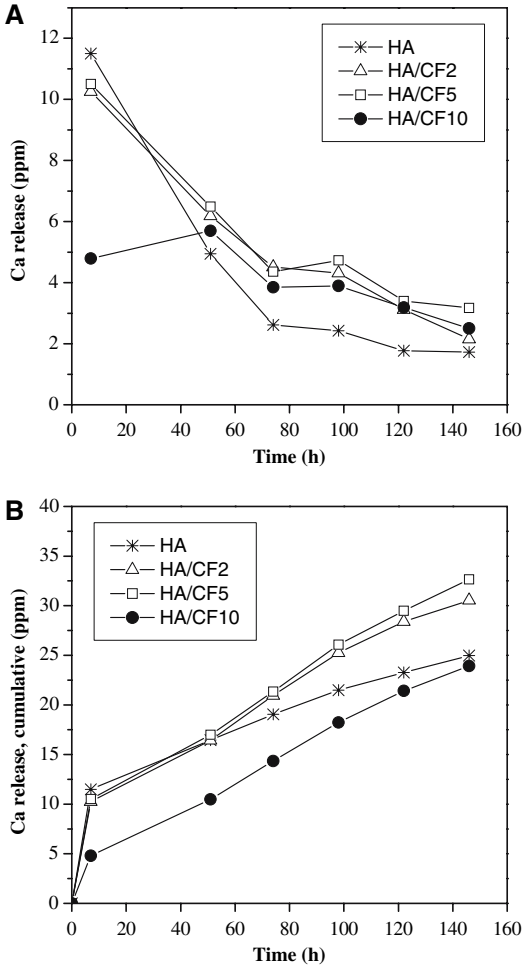

Fig. 5 (**A**) Concentration of Ca^{2+} dissolved from the apatite coatings without and with the insertion of CaF_2 layer, and (**B**) cumulative data of (**A**). Test was performed in a physiological saline solution at 37 °C

buffer layer. The concentration of Ca^{2+} released at each period from the bare apatite coating showed quite an abrupt initial increase followed by a rapid reduction with prolonged periods (Fig. 5A). However, the profile of HA/CF2 and HA/CF5 coatings showed reduced initial burst while more increased release at prolonged periods. This was more conspicuous in the HA/CF10 coatings, wherein the reduction in the initial burst effect was noticeable, and the release pattern showed quite a flattened curve, namely, more stable dissolution pattern. The released Ca at each period was plotted again in cumulative (Fig. 5B). Data showed more clearly the reduced burst effect by the insertion of CaF_2 layer, particularly in the case of HA/CF10. The initially rapid dissolution in the apatite coating is associated with the breakdown of amorphous regions. Therefore, the reduced initial burst (particularly in the case of HA/CF10) is believed to result from the increase in the crystallinity of the apatite layer and the reduction of an amorphous region.

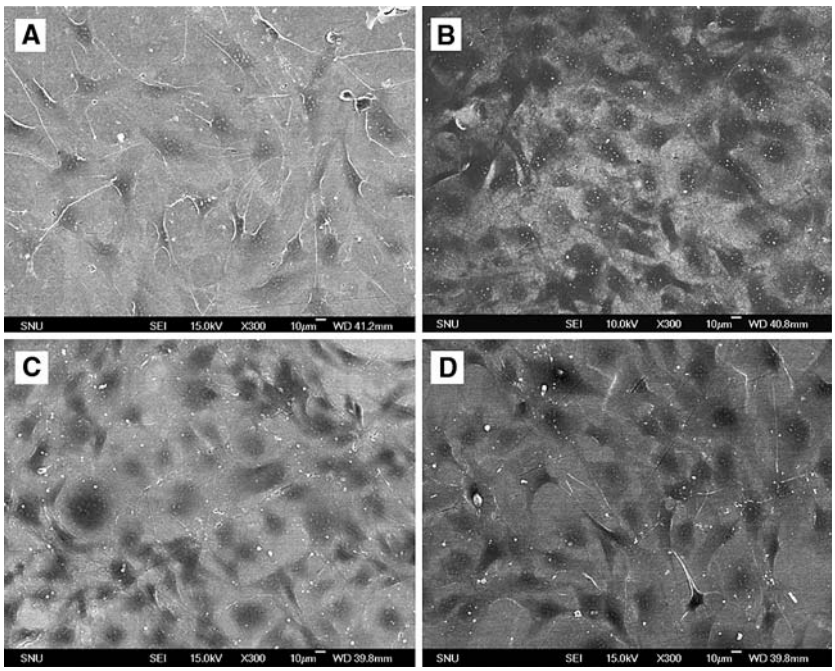

Fig. 6 Electron micrograph of the osteoblastic cells grown on the coating layer after culturing for 3 days: (**A**) HA, (**B**) HA/CF2, (**C**) HA/CF5 and (**D**) HA/CF10

Practically, the apatite coatings obtained by vaccum deposition techniques normally possess limited crystallinity even heat treated at high temperatures. In the e-beam deposited apatite also, significant level of works aimed to improve the crystallinity of the coatings as the selective dissolution of amorphous regions normally resulted in rapid disintegration of the whole coating layer [19, 20]. Therefore, the more stable dissolution profile associated with the improvement in the apatite crystallinity by the insertion of CaF_2 is preferred in terms of the issues raised above.

The CaF_2-inserted apatite coatings were observed to show favorable cell growth morphology, as shown in Fig. 6. The cells on the CaF_2-inserted apatite coatings spread well in intimate contacts with the substrate, and did not significantly alter the cytoplasmic extensions as was seen in the case of bare apatite coating. As a first criterion, this result provides the CaF_2-inserted apatite coatings did not have a considerable cytotoxic effect and may be useful in the biomedical applications. However, it is expected that the osteoblastic cells would respond quite differently to the CaF_2-inserted coatings as the significantly different dissolution profiles of the coatings, as seen in Fig. 5, may alter the ion-stimulated cellular responses [21]. Moreover, the fluoride ions existing in the underlying CaF_2 layer would be released with culturing time and consequently affect the cell behaviors [14, 16]. Therefore, in-depth cellular studies are required as a next step in order to correlate the benefits of the crystallization improvement with the biological properties.

Another consideration of the CaF_2-inserted apatite coating is the mechanical stability, which is of special importance for the applications in the load-bearing implants. The insertion of CaF_2 between the apatite and Ti creates additional interfaces, such as CaF_2/apatite and CaF_2/Ti, and this can significantly alter the mechanical properties of the coatings. Although there were no delaminations or cracks to be observed herein within the coatings or at the interfaces, further study is also warranted to confirm the mechanical stability of the newly-developed coating on Ti.

4 Conclusions

The crystallization of apatite was significantly improved by the use of CaF_2 intermediate layer in the e-beam deposition on Ti. The insertion of a thin layer (<1 μm) of CaF_2 reduced the crystallization initiation temperature of apatite as low as ~320 °C, which was in marked contrast to that (~450 °C) in the conventional apatite coating on Ti. As a result of the crystallinity improvement, the CaF_2-inserted apatite coatings, particularly the HA/CF10 coating, showed more stable dissolution profile. The morphology of the osteoblastic cells grown on the CaF_2-inserted apatite coatings was similar to that on the bare apatite coating. This new method of using CaF_2 as a buffer layer is considered potential particularly to produce apatite coatings with enhanced crystallinity and higher chemical stability.

References

1. B. Y. CHOU and E. CHANG, *J. Mater. Sci. Mater. Med.* **13** (2002) 589
2. S. OVERGAARD, K. SOBALLE, E. S. HANSEN, K. JOSEPHSEN and C. BUNGER, *J. Orthop. Res.* **14** (1996) 888

3. M. JARCHO, *Dent. Clin. North. Am.* **36** (1992) 19
4. H. W. KIM, H. E. KIM, V. SALIH and J. C. KNOWLES, *J. Biomed. Mater. Res. B* **72B** (2005) 1
5. D. M. LIU, Q. YANG, T. TROCZYNSKI and W. J. TSENG, *Biomaterials* **23** (2002) 1679
6. P. LI, *J. Biomed. Mater. Res. A* **66A** (2003) 79
7. M. WEI, A. J. RUYS, B. K. MILTHORPE and C. C. SORRELL, *J. Biomed. Mater. Res.* **45** (1999) 11
8. Y. YANG, K. H. KIM and J. L. ONG, *Biomaterials* **26** (2005) 327
9. V. NELEA, C. MOROSANU, M. ILIESCU and I. N. MIHAILESCU, *Surf. Coat. Tech.* **173** (2003) 315
10. J. M. CHOI, H. E. KIM and I. S. LEE, *Biomaterials* **21** (2000) 469
11. D. H. KIM, Y. M. KONG, S. H. LEE, I. S. LEE and H. E. KIM, *J. Am. Ceram. Soc.* **86** (2003) 186
12. E. J. LEE, S. H. LEE, H. W. KIM, Y. M. KONG and H. E. KIM, *Biomaterials* **26** (2005) 3843
13. D. SHI, G. JIANG and J. BAUER, *J. Biomed. Mater. Res. B* **63B** (2002) 71
14. S. H. LEE, H. W. KIM, Y. M. KONG, H. E. KIM, S. H. LEE and Y. I. CHANG, *J. Biomed. Mater. Res. B* **75B** (2005) 200
15. H. FATHI, A. JOHNSON, R. van NOORT, J. M. WARD and M. BROOK, *Dent. Mater.* **21** (2005) 551
16. E. J. LEE, H. W. KIM and H. E. KIM, *J. Am. Ceram. Soc.* **88**(5) (2005) 1309
17. A. CLIFFORD and R. G. HILL, *J. Non-Cryst. Sol.* **196** (1996) 346
18. D. J. WOOD and R. G. HILL, *Biomaterials* **12** (1991) 164
19. I. S. LEE, D. H. KIM, H. E. KIM, Y. C. JUN and C. H. HAN, *Biomaterials* **23** (2002) 609
20. J. M. CHOI, H. E. KIM and I. S. LEE, *Biomaterials* **21** (2000) 469
21. R. R. KUMAR and S. MARUNO, *Mater. Scie. Eng.* **A334** (2002) 156